Earth and Planetary Science Letters 409 (2015) 15–22

Contents lists available at ScienceDirect

Earth and Planetary Science Letters

www.elsevier.com/locate/epsl

Glacial cooling as inferred from marine temperature proxies TEX_{86}^{H} and $U_{37}^{K'}$

Sze Ling Ho *, Thomas Laepple

Alfred Wegener Institute, Helmholtz Centre for Polar and Marine Research, Telegrafenberg A43, D-14473 Potsdam, Germany

ARTICLE INFO

Article history:
Received 13 June 2014
Received in revised form 12 September 2014
Accepted 18 October 2014
Available online 7 November 2014
Editor: J. Lynch-Stieglitz

Keywords:
Last Glacial Maximum
sea surface temperature
multiproxy
PMIP3
$U_{37}^{K'}$
TEX_{86}^{H}

ABSTRACT

Knowledge of the magnitude of the Last Glacial Maximum (LGM) cooling is a useful constraint for estimating the climate sensitivity used in projecting future climate change. Proxy comparison, especially that between the alkenone-based $U_{37}^{K'}$ and the archaeal tetraether-based TEX_{86}, has been increasingly applied in paleoceanographic studies as a measure to better constrain proxy-derived temperature estimates. In this study, we compile and compare published multiproxy ($U_{37}^{K'}$ and TEX_{86}^{H}) records of glacial cooling measured on the same sediment cores. In spite of the diversity in oceanographic and sedimentation settings spanned by the study sites, we find that the TEX_{86}^{H}-derived mean tropical LGM cooling is approximately twice as strong as that suggested by the $U_{37}^{K'}$ and MARGO estimates. The extent of proxy discrepancy varies with the application of various regional calibrations, but the mean TEX_{86}^{H}-inferred cooling remains stronger than that inferred from $U_{37}^{K'}$. To understand the discrepancy between proxies, we examine the seasonal and water column structure of LGM cooling simulated by state-of-the-art climate models. We find that the dissimilar magnitudes of proxy-derived glacial cooling cannot be fully explained by proxies reflecting temperature of different seasons or different water depths, if the recording season and depth are assumed to stay constant through time. A hypothetical shift in recording season and/or depth between the Holocene and the LGM could in theory cause the proxy discrepancy, but this hypothesis cannot be constrained due to a lack of information on lipid production and export in the water column during the LGM. Alternatively, the systematic proxy discrepancy, which persists across diverse oceanographic settings, may imply that the commonly applied proxy calibrations for reconstructing past temperatures are fundamentally biased. As evidenced by the improved consistency between $U_{37}^{K'}$ and TEX_{86}^{H}-based estimates of LGM cooling after we applied a global subsurface (0–200 m) temperature calibration for TEX_{86}^{H}, it is plausible that the TEX_{86}^{H} signal originates from deeper in the water column than typically assumed for the proxy calibration.

1. Introduction

The climate of the Last Glacial Maximum (LGM) has been studied extensively, by means of proxy reconstructions and climate model simulations. LGM sea surface temperature estimates reconstructed from various proxies, which were compiled through community efforts such as CLIMAP (CLIMAP Project members, 1976) and MARGO (Waelbroeck et al., 2009), have been used extensively for validating climate models and constraining the climate sensitivity; a parameter relevant for the projection of future climate changes.

Previous studies have shown that the magnitude of tropical temperature change between the LGM and present day is a key parameter to constrain climate sensitivity (Hargreaves et al., 2012; Schmittner et al., 2011), i.e., the change in global surface temperature given a doubling of the atmospheric CO_2 concentration. Unfortunately, the reconstructed LGM cooling in this region was found to be proxy specific (Waelbroeck et al., 2009). Thus, an understanding of the reliability of the proxies and their differences is essential. A direct way to assess the validity of temperature estimates is to compare multiple temperature proxies from the same cores, but as the number of such datasets is limited, systematic studies comparing the regional glacial cooling are still lacking.

Earlier efforts in LGM mapping, such as CLIMAP, relied heavily on temperature estimates derived from microfossil assemblages (CLIMAP Project members, 1976). As a result of intensive development and improvement of geochemical proxies, such as

* Corresponding author. Tel.: +49 (331) 288 2187; fax: +49 (331) 288 2122.
E-mail address: Sze.Ling.Ho@awi.de (S.L. Ho).

http://dx.doi.org/10.1016/j.epsl.2014.10.033
0012-821X/

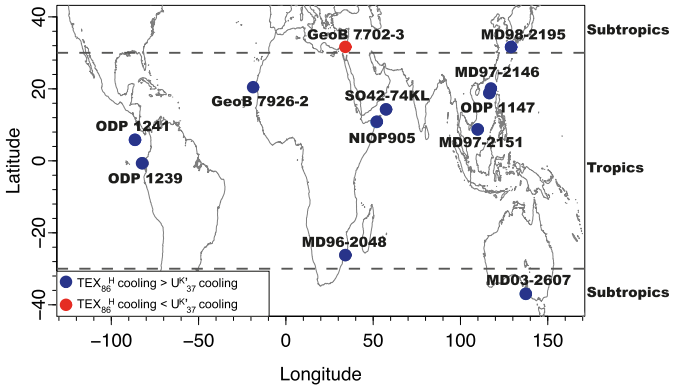

Fig. 1. Location of the study sites in our compilation and the comparison of LGM cooling derived from TEX_{86}^{H} and $U_{37}^{K'}$. Sites with stronger TEX_{86}^{H}-cooling are indicated by blue circles, whereas the site with a stronger $U_{37}^{K'}$-cooling is indicated by the red circle. The definition of tropics used in this manuscript (30°S–30°N) is shown by the dashed horizontal lines.

the alkenone-based $U_{37}^{K'}$ ($U_{37}^{K'} = [C_{37:2}]/([C_{37:2}] + [C_{37:3}])$; Prahl and Wakeham, 1987) and the Mg/Ca of planktonic foraminifera (Elderfield and Ganssen, 2000), these proxies are now routinely used to reconstruct sea surface temperature (SST) and these proxy data have been integrated in the recent MARGO database. More recently, the archaeal glycerol dialkyl glycerol tetraethers (GDGTs) based TEX_{86} (Schouten et al., 2002), and its modified counterparts, such as TEX_{86}^{H} ($TEX_{86}^{H} = Log_{10}\{([GDGT\text{-}2] + [GDGT\text{-}3] + [Crenarchaeol\ regioisomer])/([GDGT\text{-}1] + [GDGT\text{-}2] + [GDGT\text{-}3] + [Crenarchaeol\ regioisomer])\}$; Kim et al., 2010), were developed. They have been increasingly applied to reconstruct seawater temperature, especially in the tropics. Since TEX_{86} records have only recently become available, this proxy has not yet been integrated into previous mapping efforts of the LGM.

The aim of this manuscript is twofold; to present the first compilation of LGM cooling from TEX_{86}^{H} records and to examine the reliability of the cooling estimates by comparing TEX_{86}^{H} with $U_{37}^{K'}$, analyzed in tandem on the same sediment cores. As a remarkable difference was found between TEX_{86}^{H}- and $U_{37}^{K'}$-inferred LGM cooling, we use climate model simulations to test whether specific depth or season of production of the proxy source organisms could explain the observed discrepancy.

2. Approach

We compiled all published multiproxy records containing both TEX_{86}^{H} and $U_{37}^{K'}$ analyzed on the same sediment core, and spanning at least the late Holocene (0–4 kyr BP) and the LGM (19–23 kyr BP, Table 1 and Fig. 1). Nine out of the twelve sites are in the tropics (defined here as the latitudinal band between 30°N and 30°S), while the remaining three sites are from the subtropics (between 30°S and 40°S, and 30°N and 40°N).

To directly compare proxy derived temperature estimates between sites, we applied a single calibration for each proxy type. We opted for the most commonly applied global core-top calibrations: Müller et al. (1998) for $U_{37}^{K'}$ and Kim et al. (2010) for TEX_{86}^{H}. The calibration of Müller et al. (1998) is identical, within uncertainty bounds, to the calibration of Prahl et al. (1988), which is based on a laboratory culture experiment. Both the $U_{37}^{K'}$ and TEX_{86}^{H} global core-top calibrations are based on the linear correlation of the spatial pattern of sedimentary index values with climatological annual mean SSTs. We note that none of the $U_{37}^{K'}$ data in our compilation approaches the alkenone unsaturation limit of 1 (i.e. when $[C_{37:3}]$ is below detection limit), therefore the time-slice LGM cooling estimate calculated from these data are unlikely to be underestimated

Table 1
Proxy calibrations applied at the multiproxy sites and their interpretation by the original authors.

Site	Latitude (°N)	Longitude (°E)	Water depth (m)	TEX_{86}^{H} calibration	Interpretation of TEX_{86}^{H} data	$U_{37}^{K'}$ calibration	Interpretation of $U_{37}^{K'}$ data	Reference
NIOP905	10.78	51.93	1567	Schouten et al. (2002)[a]	Annual mean SST	Müller et al. (1998)	Annual mean SST	Huguet et al. (2006)
SO42-74KL	14.32	57.33	3212	Schouten et al. (2002)[a]	Annual mean SST	Müller et al. (1998)	Annual mean SST	Huguet et al. (2006)
GeoB7926-2	20.22	−18.45	2500	Kim et al. (2012)	Subsurface (0–200 m)	Müller et al. (1998)	Annual mean SST	Kim et al. (2012)
MD96-2048	−26.17	34.02	660	Kim et al. (2010)	Annual mean SST	Prahl et al. (1988)	Annual mean SST	Caley et al. (2011)
MD97-2146	20.12	117.38	1720	Kim et al. (2010)	Non-blooming season (Summer at the site)	Prahl et al. (1988)	Annual mean SST	Shintani et al. (2008, 2011)
MD97-2151	8.73	109.87	1598	Jia et al. (2012)	Subsurface (30–125 m) T	Pelejero and Grimalt (1997)	Winter SST	Yamamoto et al. (2013b)
ODP1147	18.84	116.55	3246	Schouten et al. (2003)[a]	Subsurface (75 m) T	Pelejero and Grimalt (1997)	Upper mixed layer T	Li et al. (2013)
ODP1239	−0.67	−82.08	1414	Kim et al. (2010)	Integrated surface + thermocline T	Prahl et al. (1988)	Annual mean SST	Shaari et al. (2013a)
ODP1241	5.84	−86.44	2027	Kim et al. (2010)	Integrated surface + thermocline T	Prahl et al. (1988)	Nutricline T	Shaari et al. (2013b)
GeoB7702-3	31.65	34.07	562	Kim et al. (2008)[a]	Summer T	Conte et al. (2006)	Late spring/early autumn	Castañeda et al. (2010)
MD98-2195	31.64	128.94	746	Kim et al. (2010)	T of summer thermocline	Prahl et al. (1988)	Spring SST	Ijiri et al. (2005), Kubota et al. (2010), Yamamoto et al. (2013a)
MD03-2607	−36.96	137.41	865	Kim et al. (2010)	Winter SST	Müller et al. (1998)	Annual mean SST	Lopes dos Santos et al. (2013)

Abbreviations: SST for sea surface temperature; T for temperature.
[a] TEX_{86} calibration.

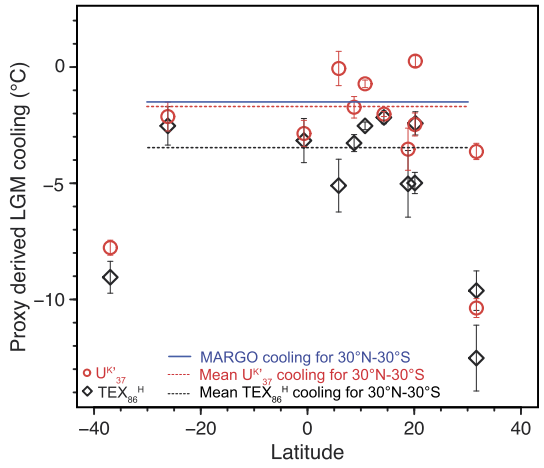

Fig. 2. Last Glacial Maximum cooling at the study sites derived from TEX_{86}^{H} and $U_{37}^{K'}$, plotted against latitude. Dashed lines indicate the mean cooling at our study sites located within the latitudinal band of 30°N and 30°S, as inferred from TEX_{86}^{H} (black) and $U_{37}^{K'}$ (red), in comparison with the MARGO estimates (blue, solid line). Error bars are the standard error of the mean. (For interpretation of the references to color in this figure legend, the reader is referred to the web version of this article.)

for approaching the upper limit of the proxy calibration (Pelejero and Calvo, 2003).

The definition of the LGM time-slice adopted here, namely 19–23 kyr BP, follows that of the CLIMAP (CLIMAP Project members, 1976) and MARGO compilations (Waelbroeck et al., 2009). Since the youngest part of most sediment records in our compilation is older than the pre-industrial (PI) period, we define the LGM cooling as the temperature anomaly between the time-slice of late Holocene 0–4 kyr BP and the LGM. This definition differs from the MARGO definition wherein the anomaly between the proxy-based LGM time-slice temperature and the instrumental-based climatological annual mean SST is reported. Our method of comparing proxy-based Holocene to proxy-based LGM values reduces biases associated with the seasonal and/or subsurface signal in proxy-derived temperature estimates, given that both the LGM and Holocene section are recording a similar season and water depth range.

As the youngest part of the sediment records in our compilation do not correspond to the same time interval, the different reference periods at different sites may lead to an additional uncertainty. However, according to the reconstructed tropical Holocene temperature evolution (Marcott et al., 2013), this uncertainty will be less than 0.2 °C (i.e. the difference between the mean of 0–4 kyr BP [−0.03 °C] and at 4 kyr BP [0.17 °C] relative to AD1961–1990 mean). We note that single measurements are susceptible to non-climate effects (e.g. Laepple and Huybers, 2013) and intrinsic climate variability, hence are not representative of the entire time period. To account for this uncertainty, we calculated the standard error of the mean of each time-slice and provide the square root of the squared sum as the total error (assuming independence of the variations in each time-slice). When fewer than three samples were available in a time-slice, we used the mean standard deviation of all other records as an estimate of the sample-to-sample variability.

3. Results and discussion

3.1. Magnitude of the LGM cooling

The reconstructed LGM cooling at the single sites range from 0.1 °C to 10.4 °C for $U_{37}^{K'}$, and from 2.2 °C and 12.5 °C for TEX_{86}^{H} (Fig. 2, and Table 2). Both proxies show a similar spatial pattern of glacial cooling ($r = 0.68$, $p < 0.01$) with a stronger cooling at the subtropical sites.

While the spatial pattern of LGM to Holocene temperature anomaly is similar between the proxies, the magnitude of the cooling is strongly proxy dependent. At eleven out of the twelve sites, the TEX_{86}^{H}-derived glacial cooling is stronger than that suggested by the $U_{37}^{K'}$ (Fig. 1). This pervasive feature ($p = 0.006$, sign-test assuming independence between sites) is unexpected given the diverse oceanographic regimes and depositional settings spanned by the study sites. The average LGM cooling based on $U_{37}^{K'}$ and TEX_{86}^{H} is 3.1 °C and 5.2 °C, respectively. Within the 30°S–30°N latitudinal band, the mean LGM cooling is 1.7 °C for $U_{37}^{K'}$ and 3.5 °C for TEX_{86}^{H}.

The mean cooling reconstructed from $U_{37}^{K'}$ for our tropical sites (1.7 °C) is within the range of $U_{37}^{K'}$-inferred LGM cooling estimates for the tropics (2 °C; Rosell-Melé et al., 2004) and for the Eastern Equatorial Pacific (1.4 °C; Dubois et al., 2009). Furthermore, compared to the TEX_{86}^{H}-derived tropical cooling, our mean $U_{37}^{K'}$-derived tropical cooling also agrees better with the MARGO estimate of 1.5 °C, which is mainly based on foraminiferal assemblages. As the LGM cooling inferred from this proxy could be biased by the habitat depth of the foraminifera (Telford et al., 2013), the MARGO cooling might be underestimated. However, re-calibrating the foraminiferal transfer function against 30–50 m to correct for the habitat depth will likely not increase the tropical cooling by more than 0.5 °C (Telford, 2014).

Composite records of $U_{37}^{K'}$ and Mg/Ca of *G. ruber*, consisting of multiple records from the eastern and western tropical Pacific, also suggest LGM cooling of no more than 2.5 °C (Timmermann et al., 2014). Furthermore, at the two sites in our compilation where concurrent foraminiferal Mg/Ca-derived and organic proxy-derived temperature records are available (namely MD96-2048 and KY07-04-01; the latter site is situated at the same location as site MD98-2195, Kubota et al., 2010), the magnitude of LGM cooling inferred from the inorganic geochemical proxy is more comparable to that of $U_{37}^{K'}$ than TEX_{86}^{H} (Table 2).

While all the foregoing estimates are closer to our $U_{37}^{K'}$ estimate, a tropical LGM cooling of 3–4 °C, comparable in magnitude to that of the TEX_{86}^{H}, is not unprecedented – especially as estimated from single site reconstructions. A cooling estimate of 3–4 °C was previously reported for the west Pacific warm pool, based on a consortium of proxies, including the clumped isotopes of planktic foraminifera and coccoliths (Tripati et al., 2014), the Mg/Ca ratio of planktic foraminifera (De Garidel-Thoron et al., 2007), and the coral Sr/Ca (Beck et al., 1992). However, it is unclear whether these estimates are site- and/or region-specific. More data are needed to demonstrate the representativeness of these reconstructions for the tropics.

Given the substantial difference between the TEX_{86}^{H}- and $U_{37}^{K'}$-based estimate of glacial cooling, it is important to resolve this issue before relying too heavily on these values in further applications, such as for the estimation of climate sensitivity. In the following sections, we will discuss several possible ways to reconcile the differences in the TEX_{86}^{H}- and $U_{37}^{K'}$-based LGM cooling estimates. These possibilities include the choice and uncertainty of the calibrations, and the hypothesis that both proxies reflect different seasons and water depths where glacial cooling might not be of the same magnitude.

3.2. Can the discrepancy be explained by the calibration choice?

Most of the $U_{37}^{K'}$ and TEX_{86}^{H} calibrations commonly used in paleoclimate reconstruction are based on the linear regressions between sedimentary proxy values and overlying SSTs. Thus, the magnitude of LGM cooling reconstructed using these linear calibrations is scaled directly by the slope of the regressions. In most

Table 2
Compilation of Last Glacial Maximum time-slice cooling inferred from TEX_{86}^{H}, $U_{37}^{K'}$ and foraminiferal Mg/Ca.

		Tropical sites (30°S–30°N)									Subtropical sites (>30°N or >30°S)		
		NIOP 905	SO42 -74KL	GeoB 7926-2	MD96 -2048	MD97 -2146	MD97 -2151	ODP 1147	ODP 1239	ODP 1241	GeoB 7702-3	MD98 -2195	MD03 -2607
Proxy													
$U_{37}^{K'}$	0–4 kyr BP n[a]	17	17	9	2	14	10	2	8	2	12	27	9
	0–4 kyr BP T (°C)	26.15	27.10	20.93	27.87	27.23	27.34	26.35	25.32	26.16	22.23	24.36	18.59
	19–23 kyr BP n	16	11	23	3	5	11	1	2	2	4	29	12
	19–23 kyr BP T (°C)	25.43	25.08	21.18	25.74	24.76	25.61	22.81	22.46	26.10	11.86	20.73	10.82
	LGM[b] ΔT (°C)	*−0.72*	*−2.02*	*0.26*	*−2.13*	*−2.47*	*−1.73*	*−3.53*	*−2.86*	*−0.06*	*−10.37*	*−3.63*	*−7.77*
	Error[c] (°C)	0.16	0.11	0.24	0.62	0.49	0.46	0.91	0.57	0.74	0.41	0.35	0.32
TEX_{86}^{H}	0–4 kyr BP n[a]	17	17	8	2	14	10	2	8	2	12	10	9
	0–4 kyr BP T (°C)	26.93	27.81	21.90	26.65	28.49	28.36	26.21	25.51	27.62	26.41	21.40	18.78
	19–23 kyr BP n	13	11	23	3	6	14	1	2	2	4	5	12
	19–23 kyr BP T (°C)	24.40	25.64	19.48	24.12	23.50	25.09	21.18	22.35	22.52	16.79	8.88	9.73
	LGM[b] ΔT (°C)	*−2.53*	*−2.17*	*−2.42*	*−2.53*	*−4.99*	*−3.27*	*−5.03*	*−3.16*	*−5.10*	*−9.62*	*−12.52*	*−9.04*
	Error[c] (°C)	0.17	0.27	0.50	0.83	0.46	0.37	1.43	0.95	1.14	0.85	1.42	0.69
Mg/Ca (*G. ruber*)	0–4 kyr BP n[a]				3							34[d]	
	0–4 kyr BP T (°C)				25.00							26.02[d]	
	19–23 kyr BP n				7							6[d,e]	
	19–23 kyr BP T (°C)				23.16							21.75[d,e]	
	LGM[b] ΔT (°C)				*−1.84*							*−4.27*	
	Error[c] (°C)				0.93							1.04	
$U_{37}^{K'}$ LGM $\Delta T - TEX_{86}^{H}$ LGM ΔT		1.81	0.15	2.68	0.4	2.52	1.54	1.5	0.3	5.04	−0.75	8.89	1.27
Mg/Ca LGM $\Delta T - U_{37}^{K'}$ LGM ΔT					0.29							−0.64	
Mg/Ca LGM $\Delta T - TEX_{86}^{H}$ LGM ΔT					0.69							8.25	

[a] n denotes the number of samples.
[b] LGM ΔT = (19–23 kyr BP T) − (0–4 kyr BP T).
[c] Standard error caused by the finite number of samples in time-slices. Error associated with calibration is discussed in section "Approach".
[d] Mg/Ca measured on core KY-04-01 retrieved from the same coordinates.
[e] Time-slice is defined as 18–23 kyr BP due to the unavailability of data older than 19 kyr BP.

of the original studies wherein proxy records in our compilation are reported, $U_{37}^{K'}$-based reconstruction were based on the calibrations of Müller et al. (1998) and Prahl et al. (1988). There are instances where regional calibrations were preferred by the authors (Table 1). One example is the South China Sea calibration of Pelejero and Grimalt (1997); the calibration was used in the original studies at sites ODP1147 (Li et al., 2013) and MD97-2151 (Yamamoto et al., 2013a, 2013b). For TEX_{86}^{H}, global calibrations are often preferred over regional calibrations, especially the latest version proposed by Kim et al. (2010). An exception is the study of Li et al. (2013), where a tropical TEX_{86} calibration (Schouten et al., 2003) was applied to reconstruct seawater temperature at site ODP 1147. Using the site-specific $U_{37}^{K'}$ and TEX_{86}^{H} calibration choice of the authors in the original publications (Tables 1 and 3) results in similar magnitude of tropical LGM cooling (1.8 °C for $U_{37}^{K'}$ and 3.5 °C for TEX_{86}^{H}) as inferred from the Müller et al. (1998) $U_{37}^{K'}$ calibration (1.7 °C) and the Kim et al. (2010) TEX_{86}^{H} calibration (3.5 °C), thus cannot explain the different cooling estimates between $U_{37}^{K'}$ and TEX_{86}^{H}.

To examine whether the above-mentioned proxy discrepancy can be potentially reconciled by the choice of alternative calibrations, we explore the possible range of LGM cooling by taking from the literature the $U_{37}^{K'}$ calibration that results in the strongest temperature change and the TEX_{86}^{H} calibration that results in the weakest temperature change. Among regional $U_{37}^{K'}$ calibrations (Table 3), the tropical Indian Ocean calibration from Sonzogni et al. (1997) yields the strongest $U_{37}^{K'}$-derived tropical LGM cooling (2.4 °C), which is 1.6 times stronger than the MARGO multiproxy estimate of 1.5 °C (for the 30°S–30°N band). Although the estimate based on the Sonzogni et al. (1997) calibration is the closest to the TEX_{86}^{H}-derived cooling of 3.5 °C, the use of this calibration at our study sites is not supported by regional $U_{37}^{K'}$ calibration studies in other tropical regions, including the South China Sea (Pelejero and Grimalt, 1997) and the Eastern Equatorial Pacific (Kienast et al., 2012), i.e. the regions where a majority of the sediment records in our compilation are located. Both of these studies found $U_{37}^{K'}$-SST sensitivities (the slope of the linear regression) that are comparable to the global calibration.

A better agreement in cooling estimates inferred from $U_{37}^{K'}$ and TEX_{86}^{H} can be achieved by applying a subsurface (0–200 m water depth) global TEX_{86}^{H} calibration (Kim et al., 2012), instead of the commonly used surface calibration (Kim et al., 2010). The subsurface calibration reduces the tropical LGM cooling from 3.5 °C to 2.6 °C, which fits within 0.9 °C with that suggested by the global $U_{37}^{K'}$ calibration (Müller et al., 1998) and would be close to a revised MARGO multiproxy estimate (Telford, 2014). Whether or not this 0.9 °C difference between $U_{37}^{K'}$ and TEX_{86}^{H} is significant depends on the (unknown) properties of the proxy uncertainty. The standard error of estimates (SEE) derived from core-top calibrations are 1.5 °C for the Müller et al. (1998) calibration and 2.2 °C for the Kim et al. (2012) calibration. While these error estimates can be directly used to assess the uncertainty in the comparison of surface sediment proxy values to modern SST it is unclear how this uncertainty may translate into the past, especially because the spatial and temporal covariance of the error is virtually unknown.

One may assume that proxy errors are independent in time and space, and in between proxies, as adopted by several recent studies (e.g., Fedorov et al., 2013; Marcott et al., 2013; Shakun et al., 2012). Under this assumption, error estimates for the temperature estimate of each time-slice are obtained by dividing the SEE by the square-root of the number of data points for each time-slice. This results in an uncertainty (1sd) of the LGM-late Holocene difference of 0.24 °C for $U_{37}^{K'}$ and 0.35 °C for TEX_{86}^{H}, rendering the 0.9 °C proxy difference in mean tropical LGM cooling significant. On the other extreme, assuming a complete

Table 3
Dependence of the $U^{K'}_{37}$- and TEX^{H}_{86}-inferred mean tropical (30°N–30°S) LGM cooling estimate on the choice of the sediment core-top calibration.

Proxy	Calibration type	Calibration reference	Mean LGM cooling (°C)
$U^{K'}_{37}$	Global	Müller et al. (1998)	1.7
	South China Sea (SCS)	Pelejero and Grimalt (1997)	1.8
	Eastern Equatorial Pacific (EEP)	Kienast et al. (2012)	1.8
	Tropical Indian Ocean	Sonzogni et al. (1997)	2.4
	Assorted (as reported in original publications)	See Table 1	1.8
TEX^{H}_{86}	Global (Calibrated against sea surface temperature at 0 m)	Kim et al. (2010)	3.5
	Global (Calibrated against seawater temperature of integrated depth of 0–200 m)	Kim et al. (2012)	2.6
	Assorted (as reported in original publications)	See Table 1	3.5

dependency of the proxy errors in time and space, i.e., the error of the average of different samples in time and space is as large as the error of a single sample (1.5 °C for $U^{K'}_{37}$ and 2.2 °C for TEX^{H}_{86}) the proxy difference of 0.9 °C cannot be considered significant. In reality the true uncertainty likely lies between the two extremes assumed here but a mechanistic understanding of processes causing the proxy uncertainty is required to provide better error estimates.

3.3. Can seasonal production and habitat depth reconcile proxy discrepancy?

3.3.1. Different seasonal production and habitat depth of TEX^{H}_{86} and $U^{K'}_{37}$

Discrepancies between proxies are often explained by invoking ecological differences, especially in terms of the seasonal production and the habitat depth of the proxy source organism (e.g., Leduc et al., 2010; Table 1). In most cases, the $U^{K'}_{37}$-derived temperature estimates are interpreted as reflecting temperature of surface mixed layer, of the annual mean or specific months, while the TEX^{H}_{86} data are considered to be reflecting either the subsurface water temperature or in rare cases, SST of specific months (Table 1). These interpretations can be in part justified by the ecology of the source organisms of the proxies. The source organisms of $U^{K'}_{37}$, namely haptophyte algae such as *E. huxleyi*, are limited to the euphotic zone where abundant sunlight is available for photosynthesis. This is not the case for TEX^{H}_{86}, whose source organism i.e. marine Thaumarchaeota, are known to occur throughout the water column (e.g. Karner et al., 2001), and in some cases the GDGTs are found to be more abundant at the subsurface than the photic zone (Sinninghe Damsté et al., 2002; Wuchter et al., 2006).

In paleoceanographic studies, interpretation of proxy data according to their ecological niche is typically constrained via the comparison of the proxy signals in surface sediments with in-situ or climatological data at the site. However, in most cases multiple explanations exist for the same surface sediment signals; for instance, a colder-than-annual-mean-SST estimate can be explained as reflecting subsurface water temperature or alternatively as sea surface temperature from colder seasons. Furthermore, in most cases, proxy data are often converted to temperature estimates using calibrations based on proxy values in surface sediments calibrated to climatological or instrumental SST, leading to a circular reasoning.

To examine whether the abovementioned seasonality and habitat depth hypotheses can result in the observed, proxy specific LGM cooling, we would need to know the depth and seasonal structure of the glacial cooling. As no observational estimates are available for the LGM, we rely on climate model simulations from the CMIP5/PMIP3 project (Braconnot et al., 2012; Taylor et al., 2012). Ocean temperature fields from preindustrial (PI) and LGM simulations of five state-of-the-art atmosphere-ocean general circulation models (AOGCMs) are analyzed by examining the monthly mean temperature at various water depths, averaged over the last 50 years of the time-slices. The five AOGCMs used here are CCSM4, CNRM-CM5, GISS-E2-R, MPI-ESM-P and MRI-CGCM3. We focus our analysis on the multi-model ensemble mean instead of single model simulation, as the former was found to be the most reliable in studies of past and future climate (e.g. Laepple et al., 2008; Lohmann et al., 2013). Furthermore, we refrain from interpreting the simulated LGM cooling in absolute values. Instead, we analyze the relative glacial cooling of different months (reported as the ratio to the annual mean cooling) and different water depths (reported as the ratio to the sea surface cooling), as these results of relative cooling should be more robust than the absolute simulated cooling.

We first analyze the hypothesis that both proxies show a different cooling as they record different seasons. In the multi-model ensemble mean, the LGM cooling of specific months (e.g. LGM June SST – PI June SST) at the sites is at most 1.25 times stronger than the annual mean LGM cooling (Fig. 3a). Therefore, if $U^{K'}_{37}$ is indeed reflecting the annual mean SST as often assumed, the discrepancy between $U^{K'}_{37}$ and TEX^{H}_{86} is unlikely to be solely attributed to TEX^{H}_{86} recording seasonal or monthly mean SST. Assuming no change in the recorded season/month between the late Holocene and LGM, even if $U^{K'}_{37}$ and TEX^{H}_{86} each record the seasons/months with the strongest and the weakest LGM cooling, respectively, the resultant amplitude of this extreme scenario is still insufficient to reconcile the differences between proxies.

The second hypothesis is that the stronger TEX^{H}_{86}-derived cooling is caused by the TEX^{H}_{86} signal reflecting subsurface temperatures. To test this hypothesis, we examine the simulated water column structure of the glacial cooling (Fig. 3b). The climate models suggest substantial spatial heterogeneity in the vertical cooling structure: at around one third of the sites (i.e. NIOP905, SO42-74KL, MD06-2048, GeoB 7702-3 and GeoB 7926-2) the subsurface cooling is stronger than the surface cooling, whereas six sites show a weaker cooling at the subsurface and one site show uniform cooling across the water column. This spatial variability is not surprising, considering the diversity of the oceanographic regimes and sedimentation settings spanned by our study sites. The strongest subsurface cooling, typically occurring at the deepest water depth examined except at site GeoB 7926-2, is on average 1.5 times stronger than that at the sea surface, but the ratio never approach the ratio of TEX^{H}_{86}-cooling over $U^{K'}_{37}$-cooling. Notably, diverging cooling patterns in the water column between sites result in a mean profile (black line in Fig. 3b) that suggests a rather homogeneous mean cooling throughout the water column. While the details of the seasonal and depth structure of the cooling differ between the individual models, the main features, i.e. the heterogeneous spatial pattern and a homogeneous cooling in the water column when averaged across sites, are found in all the single simulations. These features clearly contradict the observed discrepancy between TEX^{H}_{86} and $U^{K'}_{37}$, which shows a homogeneous spatial

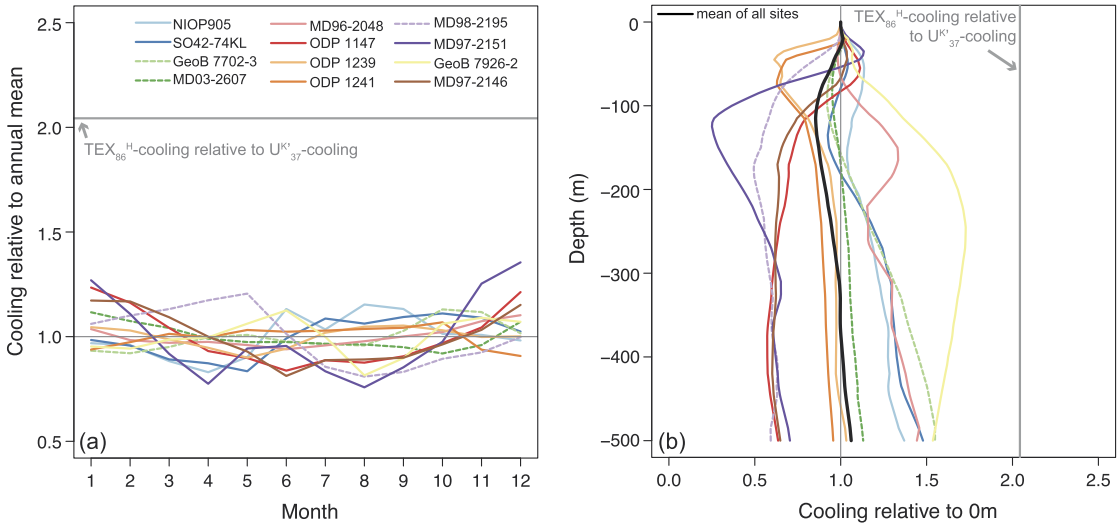

Fig. 3. Seasonal and water depth structure of the glacial cooling (LGM–Preindustrial) as simulated in the PMIP3 multi-model ensemble mean. Shown is the relative cooling (a) between the annual mean SST and monthly mean SST, and (b) between the temperature at the sea surface and the temperature at subsurface water depths. Thick gray lines indicate the observed ratio between the mean TEX_{86}^{H}-derived tropical LGM cooling and the mean $U_{37}^{K'}$-derived tropical LGM cooling. Subtropical sites are indicated by dashed lines, whereas tropical sites are indicated by solid lines.

pattern (11 of 12 sites show stronger TEX_{86}^{H}-derived cooling), and a different mean value when averaged across sites. Thus, the model simulations argue against the depth hypothesis as the cause for the systematic discrepancy between TEX_{86}^{H} and $U_{37}^{K'}$.

Further evidence against the depth hypothesis comes from Mg/Ca-derived temperature estimates measured on surface-dwelling foraminifera and subsurface-dwelling foraminifera. In both, the South China Sea and the Eastern Equatorial Pacific, the Mg/Ca data suggest that the magnitude of LGM cooling at the subsurface is either comparable (difference of 0.3 °C; Pena et al., 2008) or more attenuated compared to that at the sea surface (subsurface cooling weaker by 2 to 2.5 °C; Steinke et al., 2011, 2010), but not stronger as it would be needed to explain the stronger TEX_{86}^{H}-cooling.

3.3.2. *Temporal shifts in seasonal production over glacial–interglacial cycle?*

The seasonal and water column structure in LGM simulations suggests that the systematic discrepancy between proxies is unlikely to stem solely from proxies recording temperature of different seasons and water depths, assuming that both the recording season and water depth stay constant over time. Nevertheless, a shift in recording season from summer to winter and/or a shift to deeper depth during LGM could potentially amplify the magnitude of LGM cooling, and vice versa. For instance, a shift in alkenone production from spring in the Holocene to summer in the LGM was invoked to explain warmer-than-Holocene $U_{37}^{K'}$-derived SSTs in the subpolar regions where the alkenone production during the LGM was assumed to be limited by the availability of light (Harada et al., 2006; Rosell-Melé and Comes, 1999). In general, light availability is not a limiting factor for primary production in the tropics, and a compilation of modern day alkenone flux time series shows no evidence of alkenone flux being driven by latitudinal light availability (Rosell-Melé and Prahl, 2013), implying that the $U_{37}^{K'}$-derived LGM cooling in our compilation is unlikely to be biased by this factor. Furthermore, the small amplitude of the tropical seasonal cycle would dampen the effects of seasonality changes relative to mid and high latitudes.

Compared to haptophyte and alkenones, less is known about the archaea and the transport of their lipids to the seafloor, making it more challenging to estimate the season and depth of both the production and the export of archaeal lipids during glacial stages. In contemporary marine settings, the marine archaea seem to thrive when the primary productivity is low (Galand et al., 2010; Massana et al., 1998; Murray et al., 1998), and probably do not dwell at the sea surface because they are inhibited by high light level (Merbt et al., 2012). However, it is still unclear what primarily controls the depth and season of origin in sedimentary TEX_{86} signal. The seasonal archaeal production and the timing of carbon flux to the seafloor are probably two of the main controls, but their relative importance is expected to vary with oceanographic settings (see review by Schouten et al., 2013).

The seasonality and the export depth of the nannoplankton (of which the producers of alkenones are a subset) or picoplankton (of which the producers of GDGTs are a subset) during LGM could plausibly be constrained using models with integrated biogeochemical cycle as shown for foraminiferal proxies (Fraile et al., 2009). However, relying on such models to interpret proxy adds another layer of uncertainty especially given the current lack of understanding of the marine archaeal ecology and GDGT export mechanisms. As evidenced by the global compilation of alkenone sediment trap data (Rosell-Melé and Prahl, 2013), there is also the issue of whether or not the seasonality of the lipid flux may be directly transferred to sediments, as the seasonal signal carried by lipids can be modified during the complex sedimentation process.

In theory, the impact of a temporal shift in habitat depth or season of the proxy recorder would differ in magnitude depending on the habitat depth of the organism. This is because the vertical gradients and amplitude of seasonal cycle diminishes with water depth, so the deeper the source organism dwells the less sensitive the proxy is to seasonality/depth changes. If the TEX_{86}^{H} signals in the archaeal lipids are set at subsurface water depths, the impact of a temporal shift in recording season and/or habitat depth will be less severe on TEX_{86}^{H} records than on $U_{37}^{K'}$ records, which purportedly reflect SST. Nevertheless, a shift in recording season and/or depth would render a quantitative interpretation of the relative changes in proxy derived temperature estimates questionable, especially in terms of the often adopted approach of inferring water column structure changes using the difference between $U_{37}^{K'}$ and TEX_{86}^{H} estimates.

3.4. *Towards reconciling* $U_{37}^{K'}$ *and* TEX_{86}^{H} *discrepancy*

Given the model evidence and the large range of temperatures, latitudes and oceanographic settings spanned by the study sites,

the observed systematic difference between glacial cooling magnitude inferred from TEX_{86}^{H} and $U_{37}^{K'}$ is unlikely to be attributable to the TEX_{86}^{H} recording stronger or $U_{37}^{K'}$ recording weaker climate change. Instead, the simplest solution consistent with our finding would be that the present calibrations are biased, towards overestimating the amplitude of TEX_{86}^{H}-derived temperature changes and/or underestimating that of $U_{37}^{K'}$.

Judging from the many uncertainties in TEX_{86}^{H} calibration (Schouten et al., 2013), it is plausible that a larger proportion of the offset can be attributed to the TEX_{86}^{H}-SST calibration than the relatively well-constrained $U_{37}^{K'}$-SST calibration (see Section 3.1). Expanding the spatial coverage of the global TEX_{86}-SST calibrations does not substantially change the slope, indicating the robustness of the spatial representativeness of the existing database (Ho et al., 2014). Regressing global index values with different seasonal SST will change the intercept but not the slope of the linear regression (e.g. Müller et al., 1998). One possibility, as suggested by the reduced discrepancy in proxy comparison when using the subsurface calibration (Kim et al., 2012), is to further explore the correlation of TEX_{86}^{H} with subsurface water temperatures. As the latitudinal subsurface temperature gradients are reduced compared to that at the surface, such calibration targets can reduce the slope of regression, thereby also the amplitude of reconstructed temperatures. In addition, the proposed calibration should also be assessed in terms of consistency with downcore multiproxy evidence on a global scale and preferably on various time-scales.

4. Summary

We compiled glacial cooling estimates from $U_{37}^{K'}$ and TEX_{86}^{H} records measured on the same sediment cores. A comparison of these proxy records, in terms of the anomaly between time-slices of 0–4 kyr BP and 19–23 kyr BP, shows that the tropical LGM cooling suggested by TEX_{86}^{H} is twice as strong as the $U_{37}^{K'}$-cooling. Considering available tropical cooling estimates from other proxies and alternative calibrations, and drawing from the climate model-simulated seasonal and water depth structure, we argue that the systematic discrepancy between proxies is unlikely to stem alone from proxies recording different season or water depth. Judging from the large range of oceanographic regimes and depositional settings spanned by the study sites, it is also unlikely that the proxy discrepancy in LGM cooling stems from a concomitant shift of both proxies in recording season/depth during LGM. Instead, we contend that the seemingly overestimated magnitude of LGM cooling derived from the widely used TEX_{86}^{H}-SST global calibration is plausibly due to a biased slope of the regression, which may be improved by calibrating the index values to temperatures of water levels deeper than currently considered in the global calibration.

Acknowledgements

We are grateful to authors who made their data publicly available via NCDC and Pangaea, which greatly speed up the compilation work. We would like to thank M. Yamamoto, J.H. Kim, H. Shaari, C. Huguet, M. Zhao, L. Pena, S. Steinke, and T. Caley for sharing their published data. We gratefully acknowledge J. Groeneveld, G. Mollenhauer and the COMPARE (Comparing Ocean Models with Paleo-Archives) 2013 LGM Tropical Cooling workshop participants for insightful discussion, and T. Roy for improving the readability of this paper. Constructive reviews from two anonymous reviewers helped to further improve the manuscript. We acknowledge the World Climate Research Programme's Working Group on Coupled Modelling, which is responsible for CMIP, and we thank the climate modeling groups for producing and making available their model output. For CMIP the U.S. Department of Energy's Program for Climate Model Diagnosis and Intercomparison provides coordinating support and led development of software infrastructure in partnership with the Global Organization for Earth System Science Portals. This work is supported by the Initiative and Networking Fund of the Helmholtz Association (grant VH-NG-900).

References

Beck, J.W., Edwards, R.L., Ito, E., Taylor, F.W., Recy, J., Rougerie, F., Joannot, P., Henin, C., 1992. Sea-surface temperature from coral skeletal strontium/calcium ratios. Science 257, 644–647. http://dx.doi.org/10.1126/science.257.5070.644.

Braconnot, P., Harrison, S.P., Kageyama, M., Bartlein, P.J., Masson-Delmotte, V., Abe-Ouchi, A., Otto-Bliesner, B., Zhao, Y., 2012. Evaluation of climate models using palaeoclimatic data. Nat. Clim. Change 2, 417–424. http://dx.doi.org/10.1038/nclimate1456.

Caley, T., Kim, J.-H., Malaizé, B., Giraudeau, J., Laepple, T., Caillon, N., Charlier, K., Rebaubier, H., Rossignol, L., Castañeda, I.S., Schouten, S., Sinninghe Damsté, J.S., 2011. High-latitude obliquity as a dominant forcing in the Agulhas current system. Clim. Past 7, 1285–1296. http://dx.doi.org/10.5194/cp-7-1285-2011.

Castañeda, I.S., Schefuß, E., Pätzold, J., Sinninghe Damsté, J.S., Weldeab, S., Schouten, S., 2010. Millennial-scale sea surface temperature changes in the eastern Mediterranean (Nile River Delta region) over the last 27,000 years. Paleoceanography 25. http://dx.doi.org/10.1029/2009PA001740.

CLIMAP Project members, 1976. The Surface of the Ice-Age Earth. Science 191, 1131–1137. http://dx.doi.org/10.1126/science.191.4232.1131.

Conte, M.H., Sicre, M.-A., Rühlemann, C., Weber, J.C., Schulte, S., Schulz-Bull, D., Blanz, T., 2006. Global temperature calibration of the alkenone unsaturation index ($U_{37}^{K'}$) in surface waters and comparison with surface sediments. Geochem. Geophys. Geosyst. 7, Q02005. http://dx.doi.org/10.1029/2005GC001054.

De Garidel-Thoron, T., Rosenthal, Y., Beaufort, L., Bard, E., Sonzogni, C., Mix, A.C., 2007. A multiproxy assessment of the western equatorial Pacific hydrography during the last 30 kyr. Paleoceanography 22, PA3204. http://dx.doi.org/10.1029/2006PA001269.

Dubois, N., Kienast, M., Normandeau, C., Herbert, T.D., 2009. Eastern equatorial Pacific cold tongue during the Last Glacial Maximum as seen from alkenone paleothermometry. Paleoceanography 24, PA4207. http://dx.doi.org/10.1029/2009PA001781.

Elderfield, H., Ganssen, G., 2000. Past temperature and $\delta^{18}O$ of surface ocean waters inferred from foraminiferal Mg/Ca ratios. Nature 405, 442–445. http://dx.doi.org/10.1038/35013033.

Fedorov, A.V., Brierley, C.M., Lawrence, K.T., Liu, Z., Dekens, P.S., Ravelo, A.C., 2013. Patterns and mechanisms of early Pliocene warmth. Nature 496, 43–49.

Fraile, I., Schulz, M., Mulitza, S., Merkel, U., Prange, M., Paul, A., 2009. Modeling the seasonal distribution of planktonic foraminifera during the Last Glacial Maximum. Paleoceanography 24, PA2216. http://dx.doi.org/10.1029/2008PA001686.

Galand, P.E., Gutiérrez-Provecho, C., Massana, R., Gasol, J.M., Casamayor, E.O., 2010. Inter-annual recurrence of archaeal assemblages in the coastal NW Mediterranean Sea (Blanes Bay Microbial Observatory). Limnol. Oceanogr. 55, 2117–2125. http://dx.doi.org/10.4319/lo.2010.55.5.2117.

Harada, N., Ahagon, N., Sakamoto, T., Uchida, M., Ikehara, M., Shibata, Y., 2006. Rapid fluctuation of alkenone temperature in the southwestern Okhotsk Sea during the past 120 kyr. Glob. Planet. Change 53, 29–46. http://dx.doi.org/10.1016/j.gloplacha.2006.01.010.

Hargreaves, J.C., Annan, J.D., Yoshimori, M., Abe-Ouchi, A., 2012. Can the Last Glacial Maximum constrain climate sensitivity? Geophys. Res. Lett. 39, L24702. http://dx.doi.org/10.1029/2012GL053872.

Ho, S.L., Mollenhauer, G., Fietz, S., Martínez-Garcia, A., Lamy, F., Rueda, G., Schipper, K., Méheust, M., Rosell-Melé, A., Stein, R., Tiedemann, R., 2014. Appraisal of TEX_{86} and thermometries in subpolar and polar regions. Geochim. Cosmochim. Acta 131, 213–226. http://dx.doi.org/10.1016/j.gca.2014.01.001.

Huguet, C., Kim, J.-H., Sinninghe Damsté, J.S., Schouten, S., 2006. Reconstruction of sea surface temperature variations in the Arabian Sea over the last 23 kyr using organic proxies (TEX_{86} and $U_{37}^{K'}$). Paleoceanography 21, PA3003. http://dx.doi.org/10.1029/2005PA001215.

Ijiri, A., Wang, L., Oba, T., Kawahata, H., Huang, C.-Y., Huang, C.-Y., 2005. Paleoenvironmental changes in the northern area of the East China Sea during the past 42,000 years. Palaeogeogr. Palaeoclimatol. Palaeoecol. 219, 239–261. http://dx.doi.org/10.1016/j.palaeo.2004.12.028.

Jia, G., Zhang, J., Chen, J., Peng, P., Zhang, C., 2012. Archaeal tetraether lipids record subsurface water temperature in the South China Sea. Org. Geochem. 50, 68–77.

Karner, M.B., DeLong, E.F., Karl, D.M., 2001. Archaeal dominance in the mesopelagic zone of the Pacific Ocean. Nature 409, 507–510.

Kienast, M., MacIntyre, G., Dubois, N., Higginson, S., Normandeau, C., Chazen, C., Herbert, T.D., 2012. Alkenone unsaturation in surface sediments from the eastern equatorial Pacific: implications for SST reconstructions. Paleoceanography 27, PA1210. http://dx.doi.org/10.1029/2011PA002254.

Kim, J.-H., Schouten, S., Hopmans, E.C., Donner, B., Sinninghe Damsté, J.S., 2008. Global sediment core-top calibration of the TEX_{86} paleothermometer in the ocean. Geochim. Cosmochim. Acta 72, 1154–1173.

Kim, J.-H., van der Meer, J., Schouten, S., Helmke, P., Willmott, V., Sangiorgi, F., Koç, N., Hopmans, E.C., Damsté, J.S.S., 2010. New indices and calibrations derived from the distribution of crenarchaeal isoprenoid tetraether lipids: implications for past sea surface temperature reconstructions. Geochim. Cosmochim. Acta 74, 4639–4654. http://dx.doi.org/10.1016/j.gca.2010.05.027.

Kim, J.-H., Romero, O.E., Lohmann, G., Donner, B., Laepple, T., Haam, E., Sinninghe Damsté, J.S., 2012. Pronounced subsurface cooling of North Atlantic waters off Northwest Africa during Dansgaard–Oeschger interstadials. Earth Planet. Sci. Lett. 339–340, 95–102. http://dx.doi.org/10.1016/j.epsl.2012.05.018.

Kubota, Y., Kimoto, K., Tada, R., Oda, H., Yokoyama, Y., Matsuzaki, H., 2010. Variations of East Asian summer monsoon since the last deglaciation based on Mg/Ca and oxygen isotope of planktic foraminifera in the northern East China Sea. Paleoceanography 25, PA4205. http://dx.doi.org/10.1029/2009PA001891.

Laepple, T., Huybers, P., 2013. Reconciling discrepancies between UK37 and Mg/Ca reconstructions of Holocene marine temperature variability. Earth Planet. Sci. Lett. 375, 418–429. http://dx.doi.org/10.1016/j.epsl.2013.06.006.

Laepple, T., Jewson, S., Coughlin, K., 2008. Interannual temperature predictions using the CMIP3 multi-model ensemble mean. Geophys. Res. Lett. 35, L10701. http://dx.doi.org/10.1029/2008GL033576.

Leduc, G., Schneider, R.R., Kim, J.-H., Lohmann, G., 2010. Holocene and Eemian sea surface temperature trends as revealed by alkenone and Mg/Ca paleothermometry. Quat. Sci. Rev. 29, 989–1004. http://dx.doi.org/10.1016/j.quascirev.2010.01.004.

Li, D., Zhao, M., Tian, J., Li, L., 2013. Comparison and implication of TEX_{86} and $U^{K'}_{37}$ temperature records over the last 356 kyr of ODP Site 1147 from the northern South China Sea. Palaeogeogr. Palaeoclimatol. Palaeoecol. 376, 213–223. http://dx.doi.org/10.1016/j.palaeo.2013.02.031.

Lohmann, G., Pfeiffer, M., Laepple, T., Leduc, G., Kim, J.-H., 2013. A model–data comparison of the Holocene global sea surface temperature evolution. Clim. Past 9, 1807–1839. http://dx.doi.org/10.5194/cp-9-1807-2013.

Lopes dos Santos, R.A., Spooner, M.I., Barrows, T.T., De Deckker, P., Sinninghe Damsté, J.S., Schouten, S., 2013. Comparison of organic ($U^{K'}_{37}$, TEX^{H}_{86}, LDI) and faunal proxies (foraminiferal assemblages) for reconstruction of late Quaternary sea surface temperature variability from offshore southeastern Australia. Paleoceanography 28, 377–387. http://dx.doi.org/10.1002/palo.20035.

Marcott, S.A., Shakun, J.D., Clark, P.U., Mix, A.C., 2013. A reconstruction of regional and global temperature for the past 11,300 years. Science 339, 1198–1201. http://dx.doi.org/10.1126/science.1228026.

Massana, R., Taylor, L.T., Murray, A.E., Wu, K.Y., Jeffrey, W.H., DeLong, E.F., 1998. Vertical distribution and temporal variation of marine planktonic archaea in the Gerlache Strait, Antarctica, during early spring. Limnol. Oceanogr. 43, 607–617.

Merbt, S.N., Stahl, D.A., Casamayor, E.O., Martí, E., Nicol, G.W., Prosser, J.I., 2012. Differential photoinhibition of bacterial and archaeal ammonia oxidation. FEMS Microbiol. Lett. 327, 41–46. http://dx.doi.org/10.1111/j.1574-6968.2011.02457.x.

Müller, P.J., Kirst, G., Ruhland, G., von Storch, I., Rosell-Melé, A., 1998. Calibration of the alkenone paleotemperature index $U^{K'}_{37}$ based on core-tops from the eastern South Atlantic and the global ocean (60°N–60°S). Geochim. Cosmochim. Acta 62, 1757–1772. http://dx.doi.org/10.1016/S0016-7037(98)00097-0.

Murray, A.E., Preston, C.M., Massana, R., Taylor, L.T., Blakis, A., Wu, K., DeLong, E.F., 1998. Seasonal and spatial variability of bacterial and archaeal assemblages in the coastal waters near Anvers Island, Antarctica. Appl. Environ. Microbiol. 64, 2585–2595.

Pelejero, C., Calvo, E., 2003. The upper end of the $U^{K'}_{37}$ temperature calibration revisited. Geochem. Geophys. Geosyst. 4 (2), 1014. http://dx.doi.org/10.1029/2002GC000431.

Pelejero, C., Grimalt, J.O., 1997. The correlation between the U^{K}_{37} index and sea surface temperatures in the warm boundary: The South China Sea. Geochim. Cosmochim. Acta 61, 4789–4797.

Pena, L.D., Cacho, I., Ferretti, P., Hall, M.A., 2008. El Niño–Southern Oscillation-like variability during glacial terminations and interlatitudinal teleconnections. Paleoceanography 23, PA3101. http://dx.doi.org/10.1029/2008PA001620.

Prahl, F.G., Wakeham, S.G., 1987. Calibration of unsaturation patterns in long-chain ketone compositions for palaeotemperature assessment. Nature 330, 367–369.

Prahl, F.G., Muehlhausen, L.A., Zahnle, D.L., 1988. Further evaluation of long-chain alkenones as indicators of paleoceanographic conditions. Geochim. Cosmochim. Acta 52, 2303–2310.

Rosell-Melé, A., Comes, P., 1999. Evidence for a warm Last Glacial Maximum in the Nordic Seas or an example of shortcomings in $U^{K'}_{37}$ and U^{K}_{37} to estimate low sea surface temperature. Paleoceanography 14, 770–776.

Rosell-Melé, A., Prahl, F.G., 2013. Seasonality of temperature estimates as inferred from sediment trap data. Quat. Sci. Rev. 72, 128–136. http://dx.doi.org/10.1016/j.quascirev.2013.04.017.

Rosell-Melé, A., Bard, E., Emeis, K.-C., Grieger, B., Hewitt, C., Müller, P.J., Schneider, R.R., 2004. Sea surface temperature anomalies in the oceans at the LGM estimated from the alkenone-$U^{K'}_{37}$ index: comparison with GCMs. Geophys. Res. Lett. 31. http://dx.doi.org/10.1029/2003GL018151.

Schmittner, A., Urban, N.M., Shakun, J.D., Mahowald, N.M., Clark, P.U., Bartlein, P.J., Mix, A.C., Rosell-Melé, A., 2011. Climate sensitivity estimated from temperature reconstructions of the last glacial maximum. Science 334, 1385–1388. http://dx.doi.org/10.1126/science.1203513.

Schouten, S., Hopmans, E.C., Schefuß, E., Sinninghe Damsté, J.S., 2002. Distributional variations in marine crenarchaeotal membrane lipids: a new tool for reconstructing ancient sea water temperatures? Earth Planet. Sci. Lett. 204, 265–274. http://dx.doi.org/10.1016/S0012-821X(02)00979-2.

Schouten, S., Hopmans, E.C., Forster, A., van Breugel, Y., Kuypers, M.M., Damsté, J.S.S., 2003. Extremely high sea-surface temperatures at low latitudes during the middle Cretaceous as revealed by archaeal membrane lipids. Geology 31, 1069–1072.

Schouten, S., Hopmans, E.C., Sinninghe Damsté, J.S., 2013. The organic geochemistry of glycerol dialkyl glycerol tetraether lipids: a review. Org. Geochem. 54, 19–61. http://dx.doi.org/10.1016/j.orggeochem.2012.09.006.

Shaari, H.bin, Yamamoto, M., Irino, T., 2013a. Enhanced upwelling in the eastern equatorial Pacific at the last five glacial terminations. Palaeogeogr. Palaeoclimatol. Palaeoecol. 386, 8–15. http://dx.doi.org/10.1016/j.palaeo.2013.03.022.

Shaari, H.B., Yamamoto, M., Irino, T., Oba, T., 2013b. Nutricline shoaling in the eastern Pacific warm pool during the last two glacial maxima. J. Oceanogr. 70, 25–34. http://dx.doi.org/10.1007/s10872-013-0209-1.

Shakun, J.D., Clark, P.U., He, F., Marcott, S.A., Mix, A.C., Liu, Z., Otto-Bliesner, B., Schmittner, A., Bard, E., 2012. Global warming preceded by increasing carbon dioxide concentrations during the last deglaciation. Nature 484, 49–54.

Shintani, T., Yamamoto, M., Chen, M.-T., 2008. Slow warming of the Northern South China Sea during the last deglaciation. Terr. Atmospheric Ocean. Sci. 19, 341. http://dx.doi.org/10.3319/TAO.2008.19.4.341(IMAGES).

Shintani, T., Yamamoto, M., Chen, M.-T., 2011. Paleoenvironmental changes in the northern South China Sea over the past 28,000 years: a study of TEX_{86}-derived sea surface temperatures and terrestrial biomarkers. In: Quaternary Paleoclimate of the Western Pacific and East Asia: State of the Art and New Discovery. J. Asian Earth Sci. 40, 1221–1229. http://dx.doi.org/10.1016/j.jseaes.2010.09.013.

Sinninghe Damsté, J.S., Rijpstra, W.I.C., Hopmans, E.C., Prahl, F.G., Wakeham, S.G., Schouten, S., 2002. Distribution of membrane lipids of planktonic crenarchaeota in the Arabian Sea. Appl. Environ. Microbiol. 68, 2997–3002. http://dx.doi.org/10.1128/AEM.68.6.2997-3002.2002.

Sonzogni, C., Bard, E., Rostek, F., Dollfus, D., Rosell-Melé, A., Eglinton, G., 1997. Temperature and salinity effects on alkenone ratios measured in the surface sediments from the Indian Ocean. Quat. Res. 47, 344–355.

Steinke, S., Mohtadi, M., Groeneveld, J., Lin, L.-C., Löwemark, L., Chen, M.-T., Rendle-Bühring, R., 2010. Reconstructing the southern South China Sea upper water column structure since the Last Glacial Maximum: implications for the East Asian winter monsoon development. Paleoceanography 25, PA2219. http://dx.doi.org/10.1029/2009PA001850.

Steinke, S., Glatz, C., Mohtadi, M., Groeneveld, J., Li, Q., Jian, Z., 2011. Past dynamics of the East Asian monsoon: no inverse behaviour between the summer and winter monsoon during the Holocene. Glob. Planet. Change 78, 170–177. http://dx.doi.org/10.1016/j.gloplacha.2011.06.006.

Taylor, K.E., Stouffer, R.J., Meehl, G.A., 2012. An overview of CMIP5 and the experiment design. Bull. Am. Meteorol. Soc. 93, 485–498. http://dx.doi.org/10.1175/BAMS-D-11-00094.1.

Telford, R.J., 2014. Re-evaluating tropical LGM planktonic foraminifera assemblage-based sea-surface temperature reconstructions. Figshare. http://dx.doi.org/10.6084/m9.figshare.1014289.

Telford, R.J., Li, C., Kucera, M., 2013. Mismatch between the depth habitat of planktonic foraminifera and the calibration depth of SST transfer functions may bias reconstructions. Clim. Past 9, 859–870. http://dx.doi.org/10.5194/cp-9-859-2013.

Timmermann, A., Sachs, J., Timm, O., 2014. Assessing divergent SST behavior during the last 21 ka derived from alkenones and G. ruber-Mg/Ca in the Equatorial Pacific. Paleoceanography 29, 680–696. http://dx.doi.org/10.1002/2013PA002598.

Tripati, A.K., Sahany, S., Pittman, D., Eagle, R.A., Neelin, J.D., Mitchell, J.L., Beaufort, L., 2014. Modern and glacial tropical snowlines controlled by sea surface temperature and atmospheric mixing. Nat. Geosci. 7, 205–209. http://dx.doi.org/10.1038/ngeo2082.

Waelbroeck, C., Paul, A., Kucera, M., Rosell-Melé, A., Weinelt, M., Schneider, R., Mix, A.C., Abelmann, A., Armand, L., Bard, E., Barker, S., Barrows, T.T., Benway, H., Cacho, I., Chen, M.-T., Cortijo, E., Crosta, X., de Vernal, A., Dokken, T., Duprat, J., Elderfield, H., Eynaud, F., Gersonde, R., Hayes, A., Henry, M., Hillaire-Marcel, C., Huang, C.-C., Jansen, E., Juggins, S., Kallel, N., Kiefer, T., Kienast, M., Labeyrie, L., Leclaire, H., Londeix, L., Mangin, S., Matthiessen, J., Marret, F., Meland, M., Morey, A.E., Mulitza, S., Pflaumann, U., Pisias, N.G., Radi, T., Rochon, A., Rohling, E.J., Sbaffi, L., Schäfer-Neth, C., Solignac, S., Spero, H., Tachikawa, K., Turon, J.-L., 2009. Constraints on the magnitude and patterns of ocean cooling at the Last Glacial Maximum. Nat. Geosci. 2, 127–132. http://dx.doi.org/10.1038/ngeo411.

Wuchter, C., Schouten, S., Wakeham, S.G., Sinninghe Damsté, J.S., 2006. Archaeal tetraether membrane lipid fluxes in the northeastern Pacific and the Arabian Sea: implications for TEX_{86} paleothermometry. Paleoceanography 21, PA4208. http://dx.doi.org/10.1029/2006PA001279.

Yamamoto, M., Kishizaki, M., Oba, T., Kawahata, H., 2013a. Intense winter cooling of the surface water in the northern Okinawa Trough during the last glacial period. J. Asian Earth Sci. 69, 86–92. http://dx.doi.org/10.1016/j.jseaes.2012.06.011.

Yamamoto, M., Sai, H., Chen, M.-T., Zhao, M., 2013b. The East Asian winter monsoon variability in response to precession during the past 150 000 yr. Clim. Past 9, 2777–2788. http://dx.doi.org/10.5194/cp-9-2777-2013.